

# Annealing disorder and photoinduced order of oxygen chains in detwinned $\text{YBa}_2\text{Cu}_3\text{O}_{6.65}$ single crystals probed by Raman scattering

A. Fainstein, B. Maiorov, J. Guimpel, G. Nieva, and E. Osquiguil

*Centro Atómico Bariloche, Comisión Nacional de Energía Atómica, 8400 San Carlos de Bariloche, Rio Negro, Argentina*

(Received 25 June 1999)

Raman scattering in detwinned  $\text{YBa}_2\text{Cu}_3\text{O}_{6.65}$  single crystals is studied as a function of photoexcitation and annealing. Copper-oxygen chain-related forbidden Raman bands that are known to strongly bleach with illumination at low temperatures, increase their intensity with chain fragmentation induced by annealing at high temperature. This contrasting behavior proves the conjunction of short Cu-O fragments into longer chains on photoexcitation. We interpret the Raman modes as due to vibrations at the end of CuO chain fragments and Cu-O-Cu monomers, and use their evolution with illumination and annealing as anisotropic sensitive markers of oxygen reordering processes. The identification of the “forbidden” Raman bands is discussed in the context of our results and recent literature in the subject. We also present absorption measurements performed on  $\text{GdBa}_2\text{Cu}_3\text{O}_x$  thin films with varying oxygen content. These experiments show that the 2.2-eV absorption and the chain-related Raman peaks have different dependencies with oxygen content and illumination, ruling out an explanation that suggests that the Raman intensity reduction of these modes is due to a photobleaching of intermediate defect states. These results highlight the potentialities of Raman scattering for oxygen dynamics studies and demonstrate the presence of photoinduced oxygen ordering in these high- $T_c$  superconductor compounds.

## I. MOTIVATION

The physical properties of  $\text{YBa}_2\text{Cu}_3\text{O}_x$  depend critically upon oxygen content, and on the way in which oxygen atoms are rearranged in the basal [Cu(1)-O(1)“chain”] planes. In fact, several phases characterized by different chain order are possible and can coexist for a given oxygen content, their detailed structure being a determinant of the  $\text{CuO}_2$ -plane carrier doping and through it of the superconducting properties of the material. This structure depends on the thermal history of the sample: quenched samples show an increase of  $T_c$  with time (typically days at room temperature), which has been assigned to a reordering effect through formation of longer chains.<sup>1,2</sup> Based on transport measurements, it has been proposed that oxygen ordering can also be induced by continuous illumination, and that this effect would be at the origin<sup>3</sup> of the phenomena of persistent photoconductivity (PPC) and photoinduced superconductivity (PS).<sup>3-9</sup> Notwithstanding the years passed after the discovery of PPC and PS it has only been recently, probably motivated by the identification of some chain-related modes, that Raman-scattering experiments have been reported bringing important insight into the problem.<sup>10-12</sup>

It is known that illumination with visible or UV light induces an increase in the conductivity (PPC) and the superconducting critical temperature (PS) of oxygen-deficient  $\text{YBa}_2\text{Cu}_3\text{O}_x$ .<sup>3-9</sup> These changes are metastable if the sample is kept at temperatures below 250 K, and relax back to the equilibrium state at higher temperatures. It is generally agreed on that the phenomena are due to photodoping of the  $\text{CuO}_2$  planes by electron-hole pair excitation. The electron trapping mechanism, however, has not been conclusively established. Basically two scenarios are considered, namely photoassisted oxygen ordering<sup>3</sup> and trapping at oxygen

vacancies.<sup>8,9</sup> In the first model, the photoexcitation is thought to induce oxygen ordering into longer chains, which are known to constitute better hole dopants (and hence electron traps) than shorter fragments.<sup>13</sup> In the second model, on the other hand, the photoexcited electron is trapped into an oxygen vacancy in the Cu-O chain layer, leading to a local distortion that acts as a barrier for recombination.<sup>8,9</sup>

Raman scattering is a microscopic technique sensitive to the atomic rearrangements taking place during annealing and photoexcitation. The first report of optically induced metastabilities in the Raman spectra of detwinned  $\text{YBa}_2\text{Cu}_3\text{O}_7$  (fully oxygenated) single crystals was published in 1991.<sup>14</sup> However, at that time no complete assignment of the observed spectral features was available. The field of PPC and PS, on the other hand, had not yet fully developed.<sup>5,6</sup> An early Raman study devoted to the microscopic identification of photoinduced changes linked with PPC and PS was reported on underdoped  $\text{YBa}_2\text{Cu}_3\text{O}_{6.4}$  films.<sup>15</sup> This latter study established the reduction of the two-magnon peak associated with the antiferromagnetic order existent in the insulating phase, in agreement with the idea of photoinduced doping of the  $\text{CuO}_2$  planes. However, due to the low oxygen content of the film studied the reported spectra did not show Raman lines related to CuO-chain vibrations and thus clear signatures of photoinduced oxygen rearrangements were not detected.

We have recently reported a Raman study of photoexcitation and oxygen disorder effects on  $\text{GdBa}_2\text{Cu}_3\text{O}_x$  thin films with  $x$  ranging from 6.5 to 7.<sup>11</sup> These results rely on chain-related forbidden Raman lines assigned to vibrations at the end of Cu-O fragments.<sup>16,17</sup> Based on this assignment, the reported results provide evidence for the conjunction of short Cu-O fragments into longer chains with photoexcitation, thus strongly supporting the oxygen ordering model of PPC and

PS.<sup>3</sup> Almost at the same time, however, other Raman scattering investigations of the photoinduced metastabilities were reported.<sup>10,12</sup> Interestingly, in an alternative picture, Käll *et al.*<sup>10</sup> interpret the observation of the CuO-chain-related lines as due to a resonant Raman process mediated by electronic defect states located at the chains, without any assumption on the details of the related chain vibrations.<sup>16,17</sup> This picture heavily relies on the 2.2-eV absorption feature identification as a signature of these defect states. Thus, the conclusions drawn from the two pictures, regarding the PPC and PS phenomena, differ.

In order to test these contrasting interpretations of the observed photobleaching of Raman lines in  $\text{YBa}_2\text{Cu}_3\text{O}_x$ ,<sup>10,11</sup> we present Raman scattering experiments as a function of annealing and photoexcitation in oxygen-deficient detwinned  $\text{YBa}_2\text{Cu}_3\text{O}_{6.65}$  single crystals that extend previously reported Raman studies in  $\text{GdBa}_2\text{Cu}_3\text{O}_x$  thin films.<sup>11</sup> As compared to thin films, in detwinned single crystals the selection rules enable a more precise identification of the Raman modes. In addition, anisotropy sensitive studies of the chain oxygen dynamics are possible providing further evidence for the mode assignment and for the understanding of the physical processes under play. We also report transmission measurements performed on a series of  $\text{GdBa}_2\text{Cu}_3\text{O}_x$  thin films. We argue that the oxygen content and photoexcitation dependence of the 2.2-eV absorption is not compatible with the defect resonance interpretation of the Raman line bleaching.<sup>10</sup> These results agree with the accepted assignment of the chain-end modes<sup>11,16,17</sup> highlighting their potentialities as fragment counters in chain oxygen dynamics studies. Furthermore, we believe that they provide conclusive evidence for the contribution of chain oxygen ordering to the phenomena of PPC and PS.

The paper is organized as follows. Section II describes the samples and the experimental setup. In Sec. III we present our results and discussion, and some conclusions are bestowed.

## II. SAMPLES AND EXPERIMENTAL SETUP

The  $\text{YBa}_2\text{Cu}_3\text{O}_x$  crystal was prepared using the flux-growth technique with Ytria stabilized  $\text{ZrO}_2$  trays, as described in Ref. 18. No impurities were found in the crystal using energy dispersive spectroscopy with a scanning electron microscope. The detwinning process is done *as grown* by applying uniaxial pressure at 550 °C in an oxygen atmosphere. In a first step, oxygenation up to  $x \sim 7$  (optimal doping) was performed by annealing the crystal for 15 days at 450 °C in oxygen atmosphere. Zero-field ac susceptibility measurements showed a  $T_c$  of 92 K with 1 K superconducting transition width, as derived from the 90–10 % jump at the transition. In a latter step, the oxygen content was set so as to maximize the Raman signals due to chain-end modes. Deoxygenation down to  $x = 6.65$  was achieved by annealing the crystal for 12 days at 450 °C at a controlled oxygen pressure.<sup>19</sup> At this latter stage,  $T_c = 61$  K with a transition width of 1 K. Inspection using a microscope with polarized light showed that the crystal was well detwinned. Polarized Raman spectra (parallel and perpendicular to the CuO chains) taken with spots of  $\approx 50$   $\mu\text{m}$  diam were highly uni-

form through the crystal surface, also indicative of a well detwinned sample.

The  $\text{GdBa}_2\text{Cu}_3\text{O}_x$  thin films described here are the same used for the Raman and PPC experiments reported in Ref. 11 and Ref. 20, respectively. Fabrication details may be found there. Typical film thicknesses were around 2000 Å. The oxygen content of the samples was adjusted in a controlled manner using the isostoichiometry line annealing method.<sup>19</sup> Samples with nominal oxygen content from  $x = 6.35$  to  $x = 7$  were studied.

Raman spectra were collected with a triple Jobin-Yvon T64000 spectrometer equipped with a liquid- $\text{N}_2$ -cooled charge-coupled-device camera. The 514.5-nm line of an Ar-ion laser was used for excitation in an almost backscattering geometry. For the detwinned crystals, Raman spectra were acquired as a function of annealing with light polarized parallel or perpendicular to the Cu-O chains, and as a function of illumination time with light polarized parallel to the Cu-O chains. During the illumination periods the same laser line used for Raman data collection was also used as the light source for photoexcitation. We verified, by measuring Stokes and anti-Stokes components of the Raman spectra, that laser-induced heating of the sample was kept below  $\sim 10$ –20 K. In all cases the sample temperature and laser power density were such that changes of oxygen content due to in or out diffusion (as in Refs. 16 and 17) could be ruled out. For the absorption experiments in thin films a halogen lamp was used as light source. The transmitted light was dispersed with the Raman spectrometer and detected with a photomultiplier with conventional photon counting techniques. The scanning times and light intensity were set to avoid related photoexcitation effects. Typical resolutions were around 2–3  $\text{cm}^{-1}$  and 2 nm for the Raman scattering and the absorption spectra, respectively.

## III. RESULTS AND DISCUSSION

### A. Raman scattering

We begin describing the room-temperature ( $\sim 25$  °C) Raman spectra collected with both the  $z(a,a)\bar{z}$  and  $z(b,b)\bar{z}$  scattering configurations (labeled with Porto's notation<sup>21</sup>) in a  $\text{YBa}_2\text{Cu}_3\text{O}_{6.65}$  detwinned single crystal, and shown in Figs. 1(a) and 1(b) with thick solid curves. Spectra acquired for the sample annealed at higher temperatures are also shown in Fig. 1 and will be discussed afterwards.  $a$  and  $b$  correspond to the crystal directions perpendicular and along the Cu-O chains, respectively. The spectra are characteristic of a well-detwinned oxygen deficient  $\text{YBa}_2\text{Cu}_3\text{O}_x$  single crystal.<sup>22–25</sup> Phonon lines due to Raman-active ( $z$ )-polarized  $A_g$  symmetry modes are observed at 110  $\text{cm}^{-1}$  (Ba), 140  $\text{cm}^{-1}$  (CuO<sub>2</sub>-plane copper), 330  $\text{cm}^{-1}$  (pseudotetragonal  $B_{1g}$  symmetry CuO<sub>2</sub>-plane oxygen out-of-phase mode) and at 442  $\text{cm}^{-1}$  (CuO<sub>2</sub>-plane oxygen in-phase mode).

Besides these Raman-allowed bands many additional spectral features usually appear in oxygen-deficient  $\text{YBa}_2\text{Cu}_3\text{O}_x$  samples. Due to local changes of the atomic environment otherwise Raman-forbidden modes are activated.<sup>22–25</sup> Iliev *et al.*<sup>17</sup> have identified some of these bands as due to a superposition of the ortho-I, ortho-II, and tetragonal structures. In our spectra, the two small peaks ob-

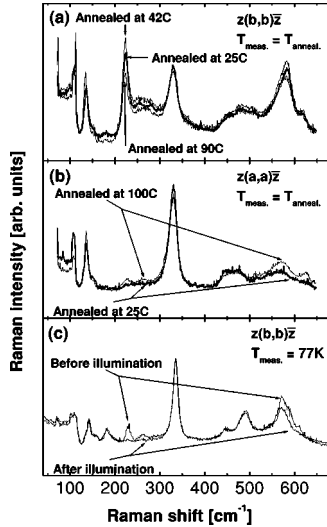


FIG. 1. Raman spectra taken under different annealing and photoexcitation conditions. (a)  $z(b,b)\bar{z}$  configuration (sensitive to the  $b$ -oriented fragments) at three different annealing temperatures. (b)  $z(a,a)\bar{z}$  configuration (sensitive to the  $a$ -oriented fragments) at two different annealing temperatures. Note the inverted intensity of the  $230$  and  $264$   $\text{cm}^{-1}$  lines with respect to the  $b$ -polarized spectra. In (a) and (b) the thicker curves correspond to the room-temperature spectra ( $25^\circ\text{C}$ ). (c)  $z(b,b)\bar{z}$  configuration before and after illumination at  $77$  K.

served at  $181$   $\text{cm}^{-1}$  and at  $495$   $\text{cm}^{-1}$  [most clear for  $z(b,b)\bar{z}$  polarization at  $77$  K, Fig. 1(c)] can be associated with ortho-II components.<sup>17</sup> The peaks that will be the subject of our research here, on the other hand, are those observed between  $220$  and  $290$   $\text{cm}^{-1}$ . Three peaks can be distinguished in our room-temperature single-crystal spectra in this spectral region: one narrow peak around  $224$   $\text{cm}^{-1}$  ( $230$   $\text{cm}^{-1}$  at  $77$  K), and two overlapping features with maxima at  $254$   $\text{cm}^{-1}$  and  $281$   $\text{cm}^{-1}$  ( $264$   $\text{cm}^{-1}$  and  $289$   $\text{cm}^{-1}$  at  $77$  K, respectively). We note that, for the thin films reported in Ref. 11, only one broad line centered around  $270$   $\text{cm}^{-1}$  could be identified instead of these latter two peaks. The three lines we will analyze are characterized by a Raman tensor with only  $\alpha_{yy} \neq 0$ , thus suggesting their connection with Cu-O chain vibrations.<sup>14</sup> In addition, the associated frequencies indicate that they are copper-related modes. For the same reasons, the large broader peak appearing also for  $z(b,b)\bar{z}$  configuration around  $580$   $\text{cm}^{-1}$  is associated with oxygen atom vibrations in finite chains.<sup>16,17</sup> However, since it is usually overlapped with a disorder-induced polarization independent signal, quantitative analysis based on it is more cumbersome.

In their pioneer work on photoinduced metastabilities on the Raman spectra of  $\text{YBa}_2\text{Cu}_3\text{O}_7$  single crystals, Wake *et al.*<sup>14</sup> showed that these chain-related modes are optically bleached for photon energies in the visible spectrum. The metastability of the photoinduced state is evidenced by the fact that, in the dark, the bleached lines reappear with a temperature-dependent recovery time indicative of an activation mechanism.<sup>10</sup> These observations were recently used in a series of Raman studies<sup>10–12</sup> devoted to understanding the microscopic origin of PPC and PS. Though all these works conclude that the CuO chains are related with the observed forbidden Raman peaks and with the PPC phenomena, the

precise assignment of the modes and the identification of the induced metastability differ. In order to clarify this central issue we have carried out Raman-scattering studies as a function of annealing, in addition to illumination. If photoinduced chain ordering is playing a role in the PPC phenomena, as proposed in Ref. 3, annealing-induced chain disorder at high temperatures should be viewed as a sort of opposed process to photoinduction.<sup>20</sup> Moreover, detwinned single crystals enable anisotropy sensitive studies that can provide further insight into the mechanisms under study.

In Fig. 1 we show such experiments performed on the  $\text{YBa}_2\text{Cu}_3\text{O}_{6.65}$  single crystal. Part (a) displays the Raman spectra obtained for  $z(b,b)\bar{z}$  configuration at different annealing temperatures. This Raman geometry is sensitive to the  $b$ -oriented chains.<sup>14</sup> Figure 1(b) shows similar spectra along  $a$  [ $z(a,a)\bar{z}$  configuration], sensitive to  $a$ -oriented chain fragments. Note that in these latter spectra the intensity of the  $230$   $\text{cm}^{-1}$  and  $264$   $\text{cm}^{-1}$  lines are inverted with respect to the  $z(b,b)\bar{z}$  configuration, showing that the signals are intrinsic to the  $a$  direction and not due to polarization leakage. Finally, spectra measured at  $77$  K before and after a long exposure to laser illumination are presented in part (c) for  $z(b,b)\bar{z}$  geometry. The chain-related modes for  $z(a,a)\bar{z}$  configuration were too weak to allow a reliable photobleaching study. Several observations can be drawn from these spectra: (i) most parts of the spectra are independent of illumination or annealing (except for some small broadenings in the latter case); (ii) changes are observed in the same spectral regions for the two processes, on the chain-related modes involving copper ( $230$ – $290$   $\text{cm}^{-1}$ ) and oxygen ( $450$ – $600$   $\text{cm}^{-1}$ ) vibrations; (iii) bleaching of these modes occurs on illumination, and an increase of their strength is observed on annealing; (iv) for these chain-related modes the intensity increases along  $a$  monotonically with annealing temperature [Fig. 1(b)], but behaves nonmonotonically along  $b$ , where an increase followed by a decrease is observed [Fig. 1(a)].

The qualitative observations discussed above are quantitatively displayed in Figs. 2 and 3. Figure 2 presents the illumination time dependence of the peak intensity for the three forbidden Raman modes assigned to chain Cu vibrations. For reference purposes, the intensity of the  $337$   $\text{cm}^{-1}$   $B_{1g}$  Raman-allowed mode is also shown. The signal intensity is defined as the peak area obtained from Lorentzian function fits to the data. While the  $B_{1g}$  mode is clearly independent of illumination time, as expected, the Cu-chain modes are optically bleached down to almost complete suppression. This result coincides with those previously reported.<sup>10–12,14</sup> In addition, it confirms our previous observation<sup>11</sup> that the forbidden mode at  $230$   $\text{cm}^{-1}$  (corresponding to the larger chain-related peak) decreases with illumination time relatively less and with a slower rate as compared with the smaller peaks around  $264$   $\text{cm}^{-1}$ .

The temperature dependence of the  $230$   $\text{cm}^{-1}$  peak intensity is shown in Fig. 3 for polarizations along  $a$  and  $b$ , and compared with the corresponding dependence of the  $B_{1g}$  mode. The  $B_{1g}$  mode integrated intensity remains constant in the studied temperature range. In contrast, the same forbidden peaks susceptible to optical bleaching display a clear anisotropic annealing temperature dependence. For light po-



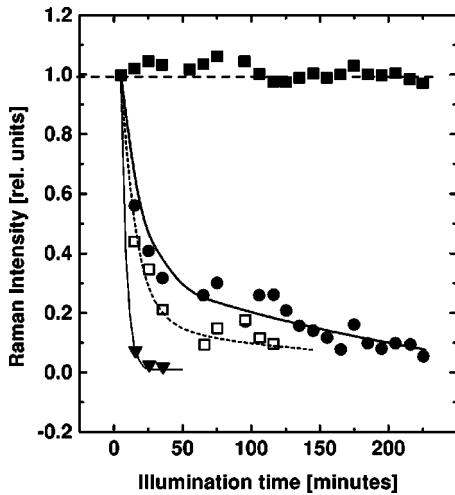


FIG. 2. Illumination time dependence of the Raman intensity (integrated area of Lorentzian fits to the data) for the  $B_{1g}$  Raman allowed peak (solid squares), and for the chain-related “forbidden” copper modes at  $230\text{ cm}^{-1}$  (full circles),  $264\text{ cm}^{-1}$  (open squares), and  $289\text{ cm}^{-1}$  (full triangles). The data correspond to spectra taken at 77 K.

larized along  $a$ , where the signals are almost unobservable under normal conditions, the forbidden modes continuously develop with increasing annealing. Along the chains ( $b$ ), on the other hand, the signal first starts increasing its strength, but decreases afterwards for larger chain disorder. We note that similar experiments performed on  $c$ -textured  $\text{GdBa}_2\text{Cu}_3\text{O}_x$  thin films showed a continuous increase of the chain modes Raman signal with annealing temperature.<sup>11</sup> We believe these results provide strong evidence of the intimate relation between chain ordering and the observed photoinduced metastabilities, and bring important information useful for the assignment of the observed modes. This discussion will be further developed below, after presenting our transmission data obtained on  $\text{GdBa}_2\text{Cu}_3\text{O}_x$  thin films as a function of oxygen concentration.

### B. Absorption

Though it is quite clear from the above-presented Raman data that the photoexcited metastability is linked to changes

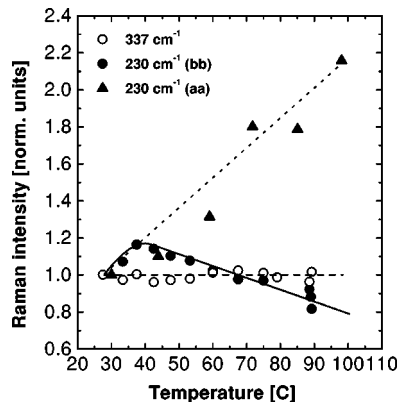


FIG. 3. Annealing temperature dependence of the Raman intensity (integrated area of Lorentzian fits to the data) for the  $B_{1g}$  Raman allowed peak (open circles), and for the chain-related “forbidden” copper modes at  $230\text{ cm}^{-1}$  in  $z(b,b)\bar{z}$  configuration (full circles) and  $z(a,a)\bar{z}$  configuration (full triangles).

in the  $\text{CuO}$ -chain basal planes, there have been two contrasting interpretations of the microscopic process involved: photoinduced ordering of the  $\text{CuO}$ -chains,<sup>11</sup> and the photoinduced reduction of the number of intermediate-step resonant electronic states.<sup>10</sup> In order to account for the oxygen-concentration dependence of the intensity of the “forbidden” Raman lines, which are maximum around  $x = 6.7$  and disappear for  $x = 6.5$  and  $x = 7$ , Käll *et al.*<sup>10</sup> concluded that the *electronic defect states* should be localized at the chain ends. This contrasts with Ref. 11 where this conclusion follows from the assignment of the *phonon modes* as being localized at chain ends.<sup>16,17</sup> Note that the stable oxygen structures for  $x = 7$  and  $x = 6.5$  are the so-called ortho-I and ortho-II structures, characterized both by infinitely long chains.<sup>11</sup> The most important fact supporting the “resonant localized state” model is the existence of a rather strong Raman resonance of the chain modes for laser excitations around  $2.2\text{ eV}$ ,<sup>14</sup> and the reported observation of a narrow absorption feature at that energy that is claimed to bleach upon illumination.<sup>26</sup> Elucidation of this point is central to the discussion, in view of the implications that each scenario has respect to the two models proposed at the origin of PPC and PS. In fact, within the scenario proposed by Käll *et al.*<sup>10</sup> no definitive conclusion can be drawn from the Raman data: the bleaching of Raman lines could be due both to the filling of intermediate defect electronic states, or to the ordering induced decrease of chain ends. The first possibility would be consistent with the vacancy model of PPC and PS (on the assumption that the chain-end electronic states are related with such trapping centers), while the second would be consistent with the photoinduced chain-ordering model.

In order to clarify this point we have performed low-temperature (80 K) transmission measurements on a series of  $\text{GdBa}_2\text{Cu}_3\text{O}_x$  thin films with nominal oxygen content ranging from  $x = 6.35$  to  $x = 7$ , before and after long exposures to high-power green laser light ( $514.5\text{ nm}$ ). The films thickness (around  $2000\text{ \AA}$ ) were such that sufficient laser illumination along the full depth sensed by the transmission measurements could be assured. Representative transmission data corresponding to some of the studied samples are displayed in Fig. 4, for the energy region of interest. A small absorption is observed around  $2.2\text{ eV}$ , that broadens and blueshifts with increasing oxygen content. This feature is clearer for  $x = 6.35$ , almost unobservable at  $x = 6.7$ , and disappears in the “fully oxygenated” sample. These observations agree with the spectroscopic ellipsometry results reported by Kircher *et al.* (see Figs. 4 and 5 in Ref. 27), and do not follow the same oxygen content dependence as the intensity of the “forbidden”  $\text{CuO}$  chain-related Raman lines. The latter are not present for  $x = 6.5$ , are well defined only for  $x > 6.5$ , have a maximum around  $x = 6.7$ , and disappear in fully oxygenated samples corresponding to  $x = 7$ .<sup>10,11</sup> Moreover, we have not observed within our experimental error any difference of the absorption spectra taken before and after laser-light illumination. An example of this is shown in Fig. 4 for  $x = 6.35$ .

### C. Discussion

Two related issues need to be discussed: first, the assignment of the additional Raman lines in the spectral region

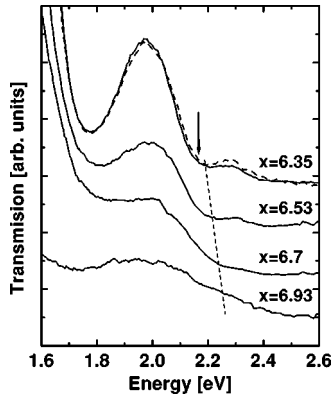


FIG. 4. Transmission spectra taken at 77 K for  $\text{GdBa}_2\text{Cu}_3\text{O}_x$  thin films of different oxygen content. Note the small absorption observed around 2.2 eV, probably associated with the “yellow resonance” (Ref. 14) of the CuO-chain-related additional modes. The dashed curve was taken without moving the sample after a long exposure to green laser light. No difference in the absorption spectra, within experimental error, was observed before and after illumination.

$230\text{--}290\text{ cm}^{-1}$  and, second, the description of the observed annealing and photoexcitation dependencies of these peaks based on this assignment, and its implications concerning the microscopic mechanism for the phenomena of PPC and PS.

In the most recent publications on the subject, basically two assignments have been given to explain the appearance of these additional lines, namely, vibrations of copper atoms localized at the end of *short* chain fragments,<sup>16,17</sup> and infrared-active chain vibrations made Raman active by resonant processes at *electronic states* localized at chain ends.<sup>10</sup> Several of our results can be used to discard this second option: (i) an absorption is, in fact, observed around 2.2 eV that could be related with the electronic intermediate states responsible for the resonant behavior of the Raman efficiency, but its variation with oxygen content and illumination *cannot* account for the respective dependencies of the Raman lines; (ii) we have observed that both in thin films<sup>11</sup> and single crystals, the additional “forbidden” modes increase their intensity with increasing temperature, something difficult to explain from the point of view of resonant processes. Though it is true that the number of chain ends increases with disorder, any resonant process should be washed out by the reduced lifetime of the intermediate electronic states. The latter is determined by the movement of oxygen atoms within the CuO planes, and is known to be drastically shortened above room temperature.<sup>3,20</sup> We hence conclude that the photobleaching of the Raman peaks cannot be due to the variation of the number of intermediate resonant states responsible for the yellow resonance.<sup>14</sup>

The peaks under consideration have been recently assigned to  $A_g$ -symmetry stretching vibrations of copper atoms at the end of *short* chain fragments.<sup>16,17</sup> Within this picture, these modes become Raman active in oxygen-deficient  $\text{YBa}_2\text{Cu}_3\text{O}_x$  due to the loss of inversion symmetry of the atomic sites, and are thus forbidden for infinite (or long with respect to the laser wavelength) chains. This identification, confirmed by detailed studies of local oxygen arrangements (microdomains),<sup>17</sup> is based on several observations. First, a site-selective isotopic substitution of *tetragonal*

$\text{YBa}_2\text{Cu}_3^{18}\text{O}_{6.2}$  microcrystals with  $^{16}\text{O}$ , indicates that a peak in the same spectral region appears upon the incorporation of oxygen atoms at the chain sites, disappearing later for increasing mean chain lengths.<sup>16</sup> A group theory analysis of the proposed Cu-O chain fragment modes can be found in Ref. 16. Second, this assignment is also consistent with the copper and oxygen Raman-allowed vibrations of the *double* Cu-O chains of the “124”  $\text{YBa}_2\text{Cu}_4\text{O}_8$  compound,<sup>28</sup> observed around  $250\text{ cm}^{-1}$ . Third, these modes have maximum intensity around  $x=6.7$ , and are not observed for  $x=6.5$  and  $x=7$ , for which the most stable ortho-II and ortho-I structures, respectively, are characterized by infinitely long chains. All vibrations involving the movement of atoms in these “infinite” chains are Raman forbidden.<sup>21,22</sup> The reason for the activation of these modes in finite fragments can be easily explained in a practical way starting from a bond-polarizability model (BPM), as explained in Ref. 11. The BPM implies that the main part of the observed Raman signal arises from vibrations of the atoms at the end of Cu-O fragments, the other neighbors contributing with rapidly decreasing intensities.<sup>11</sup> It follows that the magnitude of these modes can be used as a *counter* of chain fragments.

The above picture is able to explain the appearance of Raman signals in the spectral region around  $250\text{ cm}^{-1}$ . It is not sufficient, however, to describe the details of the spectra, which are characterized not by one, but a series of well-defined peaks. For samples of different origins the number of peaks is not always the same, but they are always *at the same* frequencies. The most prominent one is observed at room temperature around  $230\text{ cm}^{-1}$ , smaller ones appearing at  $260, 290,$  and  $305\text{ cm}^{-1}$ .<sup>10–12,24</sup> The relative intensities of these secondary peaks, on the other hand, do not follow a general rule. Panfilov *et al.*<sup>12</sup> have proposed that they are due to local ordered chain arrangements leading to a folding of the infrared-active chain mode dispersion and thus to an activation of new  $k=0$  modes. Such kind of folding is well known to occur and leads to new observable Raman modes in, for example, artificially grown semiconductor multiple quantum wells.<sup>29</sup> It is difficult to reconcile, however, this description for the additional peaks with the experimental observations noted above and our annealing results: first, a new periodicity common to all the studied samples with different oxygen contents would be required to account for the universally observed phonon frequencies. Second, if present, the folding periodicity and consequently, the Raman modes, should disappear with annealing induced disorder, in contrast with our observations (see Fig. 1 and Ref. 11). Third, the stretching chain modes should have a negative  $k$  dispersion so that the folded modes should have *lower*, and not higher, energy compared with the main  $230\text{-cm}^{-1}$  vibration. And fourth, the relative intensity of the observed peaks does not agree with the expected decay for increasing folded mode order.<sup>29</sup> Note, in particular, that in our spectra polarized along  $a$  [Fig. 1(b)] the relative intensities are *reversed*.

We have proposed in Ref. 11 a tentative assignment for the Raman peaks observed in our  $\text{GdBa}_2\text{Cu}_3\text{O}_x$  thin film experiments. In these films, in addition to the larger line at  $230\text{ cm}^{-1}$ , a single broader peak was observed around  $270\text{ cm}^{-1}$ . We suggested, following Ivanov *et al.*,<sup>16,17</sup> that the main line derives from copper atoms vibrating at the end of finite fragments, while the broader higher-frequency peak re-

flects an unresolved series of closely lying frequencies arising from monomers in different local environments (occupied or unoccupied neighbor oxygen sites, coupling to other monomers, etc.). A “monomer” is defined by the shortest possible fragment, i.e., Cu-O-Cu. We believe this is a plausible explanation that can be extended to account for the richer single-crystal spectra. In fact, irrespective of the oxygen concentration all these Cu-O arrangements should be present,<sup>16,17</sup> and might be spectrally discernible in high-quality single crystals. We believe that the somewhat larger sensitivity of the additional smaller peaks to photoexcitation, together with the observation of their larger intensity for the  $z(a,a)\bar{z}$  configuration as compared with the 230-cm<sup>-1</sup> peak, are also consistent with this scenario. Unfortunately, no reliable calculation of Cu-O fragment or cluster phonon frequencies in oxygen-deficient YBa<sub>2</sub>Cu<sub>3</sub>O<sub>x</sub> are available at the moment to firmly establish this point. Such results would greatly enhance the potentialities of Raman scattering for oxygen-dynamics studies in these compounds.

Having established the assignment of the larger 230-cm<sup>-1</sup> line as originating from vibrations at the end of chain fragments,<sup>11,16,17</sup> and thus its intensity as a sort of “fragment counter,” several facts can be drawn from the experiments. First, our results demonstrate the connection between both thermal treatment (annealing above room temperatures at constant oxygen content) and illumination with laser light: it is quite clear that *the same spectral features* suffer changes upon annealing or illumination. Second, the data in Figs. 2 and 3 serve to follow the evolution of the chain fragment distribution during the two processes. It can thus be firmly established that short Cu-O fragments conjoin into longer chains with photoexcitation, and that the long fragments break into shorter ones with annealing at increasing temperatures. The latter conclusion is the counterpart of the well-known oxygen reordering effect that favors the formation of longer chains in samples quenched from high to room temperature.<sup>1,2</sup> To be more precise, the above conclusion could be viewed as a quite general implication of our Raman data, irrespective of any line assignment: the additional “forbidden” peaks increase their strength with annealing induced disorder<sup>11</sup> and, consequently, their bleaching with illumination reflects the underlying photoinduced oxygen ordering. This reordering has been previously monitored through Raman scattering in a rather indirect way by analyzing the line shape of the Raman-allowed band due to the *neighbor apical-oxygen* vibrations.<sup>30,31</sup> Use of specific local probes such as the chain modes we are discussing here, clearly provides a new and more precise means to study such processes. We note that the conjunction of short fragments into larger ones upon photoexcitation, supports the role of oxygen ordering in the PPC and PS phenomena.<sup>3-9</sup> As proposed by

Osquiguil *et al.*,<sup>3</sup> extra charge is transferred to the conducting CuO<sub>2</sub> planes by photoinduced oxygen ordering, thus generating a metastable state with lower resistivity (PPC) and higher superconducting transition  $T_c$  (PS).

Knowledge of the vibrations involved in the Raman peaks, however, enables a much richer view into the microscopic processes under play. As argued above, the larger peak at 230 cm<sup>-1</sup> due to phonons involving the Cu atoms at the end of chain fragments, can be used through an appropriate modeling as a probe of the fragment distribution. It is interesting in this context to discuss the anisotropic behavior displayed in Fig. 3. Unfortunately, we do not have reliable data on monomers, but a mechanism of redistribution of oxygen ions between an *a* and *b* direction, as well as between long chain fragments and monomers, might be as follows. As a function of annealing temperature, the first increase of the 230-cm<sup>-1</sup> line intensity for light polarized along *b* implies a fragmentation of long chains into shorter fragments and, as indicated by the *a* spectra, movement of single oxygen atoms to the orthogonal vacant sites along *a*. On increased annealing induced disorder, however, the number of long chain fragments along *b* should start decreasing in favor of increased number of monomers. This should result in a decrease of the signal intensity along *b*, while the signal along *a* should keep increasing, as observed. This rather qualitative description considers the Raman line intensity as directly proportional to the fragment number. It would be highly desirable, however, to have a more detailed description of the dependence of the Raman process on the chain length, a dependence not taken into account in our crude approach.

In summary, we have presented a Raman-scattering study in a detwinned YBa<sub>2</sub>Cu<sub>3</sub>O<sub>6.65</sub> single crystal as a function of photoexcitation and annealing at constant oxygen content that demonstrates the intimate connection between persistent photoconductivity and photoinduced oxygen ordering in these superconductor compounds. We hope these results stimulate theoretical work on the phonon frequencies and Raman efficiencies of CuO chain fragments with different surroundings. Raman scattering would hence be a much more powerful tool for probing the concentration dependence of the oxygen local order and diffusivity<sup>32</sup> in the YBa<sub>2</sub>Cu<sub>3</sub>O<sub>x</sub> family of compounds.

#### ACKNOWLEDGMENTS

Special thanks are due to J. Azcarate and S. A. Grigera for help during sample preparation. Discussions with S. Valenzuela, P. Etchegoin, and R. G. Pregliasco are also acknowledged. This work was partially supported by ANPCYT PICT97 03-00061-01116 and PICT97 03-00061-01117, Fundación Antorchas, Fundación Balseiro, and CONICET. J.G., E.O., and G.N. are also members of CONICET, Argentina.

<sup>1</sup>B. W. Veal, A. P. Paulikas, H. Shi, Y. Fang, and J. W. Downey, Phys. Rev. B **42**, 6305 (1990).

<sup>2</sup>J. Kircher, E. Brücher, E. Schönherr, R. K. Kremer, and M. Cardona, Phys. Rev. B **46**, 588 (1992).

<sup>3</sup>E. Osquiguil, M. Maenhoudt, B. Wuyts, Y. Bruynseraede, D. Lederman, and I. K. Schuller, Phys. Rev. B **49**, 3675 (1994).

<sup>4</sup>A. I. Kirilyuk, N. M. Kreines, and V. I. Kudinov, Pis'ma Zh. Éksp. Teor. Fiz. **52**, 696 (1990) [JETP Lett. **52**, 49 (1990)].

<sup>5</sup>G. Nieva, E. Osquiguil, J. Guimpel, M. Maenhoudt, B. Wuyts, Y. Bruynseraede, M. P. Maple, and I. K. Schuller, Phys. Rev. B **46**, 14 249 (1992); Appl. Phys. Lett. **60**, 2159 (1992).

<sup>6</sup>V. I. Kudinov, I. L. Chaplygin, A. I. Kirilyuk, N. M. Kreines, R.

- Laiho, E. Lähderanta, and C. Ayache, *Phys. Rev. B* **47**, 9017 (1993), and references therein.
- <sup>7</sup>Y. H. Kim, C. M. Foster, A. J. Heeger, S. Cox, and G. Stucky, *Phys. Rev. B* **38**, 6478 (1988).
- <sup>8</sup>J. F. Federici, D. Chew, B. Welker, W. Savin, J. Gutierrez-Solana, T. Fink, and W. Wilber, *Phys. Rev. B* **52**, 15 592 (1995).
- <sup>9</sup>T. Endo, A. Hoffmann, J. Santamaria, and I. Schuller, *Phys. Rev. B* **54**, R3750 (1996).
- <sup>10</sup>M. Käll, M. Osada, M. Kakihana, L. Börjesson, T. Frello, J. Madsen, N. H. Andersen, R. Liang, P. Dosanjh, and W. N. Hardy, *Phys. Rev. B* **57**, R14 072 (1998).
- <sup>11</sup>A. Fainstein, P. Etchegoin, and J. Guimpel, *Phys. Rev. B* **58**, 9433 (1998).
- <sup>12</sup>A. G. Panfilov, A. I. Rykov, S. Tajima, and A. Yamanaka, *Phys. Rev. B* **58**, 12 459 (1998).
- <sup>13</sup>G. Uimin, *Phys. Rev. B* **50**, 9531 (1994), and references therein.
- <sup>14</sup>D. R. Wake, F. Slakey, M. V. Klein, J. P. Price, and D. M. Ginsberg, *Phys. Rev. Lett.* **67**, 3728 (1991).
- <sup>15</sup>J. Watte, G. Els, C. Andrzejak, G. Güntherodt, V. V. Moshchalkov, B. Wuyts, M. Maenhoudt, E. Osquiguil, R. E. Silverans, and Y. Bruynseraede, *J. Supercond.* **7**, 131 (1994).
- <sup>16</sup>V. G. Ivanov, M. N. Iliev, and C. Thomsen, *Phys. Rev. B* **52**, 13 652 (1995).
- <sup>17</sup>M. N. Iliev, H.-U. Habermeier, M. Cardona, V. G. Hadjiev, and R. Gajic, *Physica C* **279**, 63 (1997); M. N. Iliev, P. X. Zhang, H.-U. Habermeier, and M. Cardona, *J. Alloys Compd.* **251**, 99 (1997).
- <sup>18</sup>E. F. Righi, S. A. Grigera, G. Nieva, and F. de la Cruz, *Supercond. Rev.* **2**, 205 (1998).
- <sup>19</sup>E. Osquiguil, M. Maenhoudt, B. Wuyts, and Y. Bruynseraede, *Appl. Phys. Lett.* **60**, 2159 (1992).
- <sup>20</sup>J. Guimpel, B. Maiorov, E. Osquiguil, G. Nieva, and F. Pardo, *Phys. Rev. B* **56**, 3552 (1997).
- <sup>21</sup>M. Cardona, in *Light Scattering in Solids*, edited by M. Cardona and G. Güntherodt (Springer, Berlin, 1982), Vol. 2.
- <sup>22</sup>C. Thomsen, in *Light Scattering in High- $T_c$  Superconductors*, edited by M. Cardona and G. Güntherodt, *Topics in Applied Physics* Vol. 68 (Springer, Berlin, 1991), pp. 285–359.
- <sup>23</sup>C. Thomsen and M. Cardona, in *Physical Properties of High-Temperature Superconductors*, edited by D. M. Ginsberg (World Scientific, Singapore, 1989), Vol. I, p. 409.
- <sup>24</sup>R. Liu, C. Thomsen, W. Kress, M. Cardona, B. Gegenheimer, F. W. de Wette, J. Prade, A. D. Kulkarni, and U. Schröder, *Phys. Rev. B* **37**, 7971 (1988).
- <sup>25</sup>C. Thomsen, M. Cardona, B. Gegenheimer, R. Liu, and A. Simon, *Phys. Rev. B* **37**, 9860 (1988).
- <sup>26</sup>V. M. Dimitriev, V. V. Eremenko, V. G. Piryatinskaya, O. R. Prikhod'ko, and E. V. Khristenko, *Fiz. Nizk. Temp.* **19**, 1364 (1993) [*Low Temp. Phys.* **19**, 968 (1993)].
- <sup>27</sup>J. Kircher, M. K. Kelly, S. Rashkeev, M. Alouani, D. Fuchs, and M. Cardona, *Phys. Rev. B* **44**, 217 (1991).
- <sup>28</sup>E. T. Heyen, R. Liu, C. Thomsen, R. Kremer, and M. Cardona, *Phys. Rev. B* **41**, 11 058 (1990).
- <sup>29</sup>For a review, see, for example, B. Jusserand and M. Cardona, in *Light Scattering in Solids*, edited by M. Cardona and G. Güntherodt, *Topics in Applied Physics* Vol. 66 (Springer, Berlin, 1989), pp. 49–152.
- <sup>30</sup>V. G. Hadjiev, C. Thomsen, J. Kircher, and M. Cardona, *Phys. Rev. B* **47**, 9148 (1993).
- <sup>31</sup>M. Iliev, C. Thomsen, V. Hadjiev, and M. Cardona, *Phys. Rev. B* **47**, 12 341 (1993).
- <sup>32</sup>V. Dediu and F. C. Matocotta, *Phys. Rev. B* **57**, 7514 (1998).